

Inclined yield lines in flange outstands

M.R. Bambach[†]

Department of Civil Engineering, Monash University, VIC 3800, Australia

(Received November 27, 2006, Accepted May 23, 2008)

Abstract. While spatial plastic mechanism analysis has been widely and successfully applied to thin-walled steel structures to analyse the post-failure behaviour of sections and connections, there remains some contention in the literature as to the basic capacity of an inclined yield line. The simple inclined hinge commonly forms as part of the more complex spatial mechanism, which may involve a number of hinges perpendicular or inclined to the direction of thrust. In this paper some of the existing theories are compared with single inclined yield lines that form in flange outstands, by comparing the theories with plate tests of plates simply supported on three sides with the remaining (longitudinal) edge free. The existing mechanism theories do not account for different in-plane displacement gradients of the loaded edge, nor the slenderness of the plates, and produce conservative results. A modified theory is presented whereby uniform and non-uniform in-plane displacements of the loaded edge of the flange, and the slenderness of the flange, are accounted for. The modified theory is shown to compare well with the plate test data, and its application to flanges that are components of sections in compression and/or bending is presented.

Keywords: inclined yield lines; spatial plastic mechanisms; post-failure behaviour; plastic hinge capacity; unstiffened plates; flange outstands.

1. Introduction

It is well understood that for thin-walled steel members under increasing load, localisation of the buckling pattern occurs and the post-buckling behaviour is characterised by large local displacements in the inelastic range, which produces plastic folding of the cross-sections walls, and the member falls into a spatial plastic mechanism. In analysing thin-walled steel members a generalised spatial mechanism analysis, which takes into account second-order effects, will produce a load-deformation relationship. The first step of such a procedure is to correctly identify the spatial plastic mechanism that forms in the member, for which experimental observations have been found to be the most reliable method, however Mahendran and Murray (1991) and Mahendran (1997) have shown that some general relationships between cross-section geometry and initial imperfections may be used to assist in predicting the type of spatial plastic mechanism that will form. In practice it has been observed that there are two major classes of spatial plastic mechanisms that form in steel members, namely true mechanisms and quasi-mechanisms. A true mechanism is one whereby the component plates of the cross-section fold along the plastic hinge lines, whereas in a quasi-mechanism certain zones of the plates must deform in-plane in order for the plastic

[†] Ph.D., E-mail: mike.bambach@eng.monash.edu.au

mechanism to develop, resulting in yield zones in addition to yield lines. Murray and Khoo (1981) and Murray (1984) noted that for true mechanisms to form, it is assumed that the component plates of the cross-section can twist freely at right angles to the direction of thrust, for non-symmetric hinges. Having established the spatial plastic mechanism, the analysis follows either an energy or an equilibrium approach. The energy method derives the equilibrium condition by equating the work of external loads to the work dissipated by the mechanism during a kinematically admissible displacement, and may be applied to stationary or rolling yield lines. The equilibrium method derives the equilibrium condition from consideration of equilibrium in infinitesimal width arbitrary strips parallel to the direction of thrust, and may only be applied to stationary yield lines. The equilibrium approach is generally mathematically simpler and has been used more widely than the energy approach in the analysis of steel members and connections.

Much research effort has occurred since the early work of Murray and Khoo (1981) and Murray (1973, 1984) in order to determine and analyse the spatial plastic mechanisms that form in steel members and connections, such as plates, stiffened plates, open sections (I-sections, plain channel sections, lipped channel sections, Z-sections), closed sections (square, rectangular, triangular, trapezoidal, circular, hat, double skinned squares, ring-stiffened cylinders, conical shells, foam-timber- and concrete-filled box sections), connections (plate to closed section connections, closed section T, X and K connections) and ductility and energy absorption studies (closed sections, foam filled closed sections). It is not the purpose of this paper to review this work, and the interested reader is referred to the extensive review of Zhao (2003) which describes and references 89 papers published in the field. The spatial plastic mechanisms that form in the various members and connections consist of yield lines forming in the various component plates, often in quite complicated patterns, and may also involve zones of in-plane yielding. In many cases the yield lines that form are inclined to the direction of thrust, and thus a fundamental requirement of the analysis is to determine the reduced plastic moment capacity of an inclined yield line. This paper is concerned with the determination of the capacity of inclined yield lines that form in flange outstands of open thin-walled steel sections, and how this capacity varies with both the in-plane rotation that occurs at the loaded ends of the flange outstands, and with the slenderness of the flange outstand.

2. Inclined yield line mechanism theory

A number of authors have developed statical solutions for inclined yield lines, and have used different assumptions for both the stress distribution and the enforcement or not of a yield criterion. Early efforts include those by Murray and Khoo (1981), Murray (1984), Davies, Kemp and Walker (1975) and Mouty (1976), however none of the stress distributions were statically admissible since the twisting moment was ignored (M_t in Fig. 1), which thus violated the equilibrium condition. More recent models have enforced either von Mises or Tresca yield criteria such as those by Bakker (1990), Zhao and Hancock (1993a,b), Cao *et al.* (1998), Rhodes (2002) and most recently Hiriyur and Schafer (2005), however only Zhao and Hancock explicitly included the effect of the twisting moment on the stress distribution. Comparisons of the various formulae in Zhao and Hancock (1993b), Cao *et al.* (1998) and Hiriyur and Schafer (2005) show that they produce quite different results. In this paper selected methods are compared with test results of single inclined yield lines that formed in the unstiffened plate tests of Bambach and Rasmussen (2004a). The

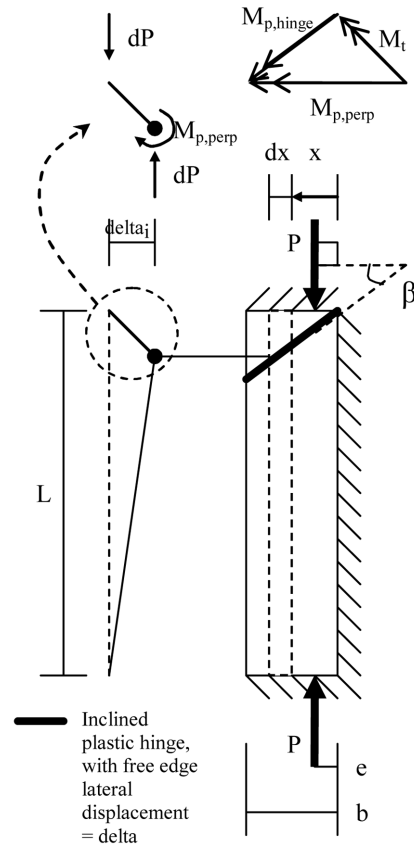


Fig. 1 Single inclined yield line formed in an unstiffened plate with three sides simply supported and the remaining (longitudinal) edge free

unstiffened plate tests consisted of rectangular plates simply supported on three sides with the remaining (longitudinal) edge free, under uniform and non-uniform in-plane compression. The selected methods are the original method of Murray and Khoo (1981) (Eq. (1)), the simplified method of Zhao and Hancock (1993b) (Eq. (2)), and Hiriyur and Schafer's (2005) modification of the Bakker (1990) method (Eqs. (3) and (4)). Hiriyur and Schafer (2005) built upon the Bakker method and satisfied the von Mises yield criterion. The rigorous method of Zhao and Hancock (1993a,b) was verified against test results of single inclined hinges, however the solution was iterative rather than explicit and quite complicated, particularly considering that in the analysis of flange outstands one must iterate across the plate width (see the next section) and an explicit solution is therefore mathematically much simpler. The simplified solution proposed by Zhao and Hancock (1993b) was shown to be almost as accurate as the iterative one, and is thus acceptable for this analysis. It is shown in Figs. 7-9 that although the various methods for calculating the capacity of the inclined yield line are quite different, in application to yield lines forming in flange outstands the results are quite similar.

Murray and Khoo (1981)
$$M_{p,hinge} = \frac{b}{\cos \beta} \frac{f_y t^2}{4} \left[1 - \left(\frac{P}{f_y b t} \right)^2 \right] \quad (1)$$

$$\text{Zhao simplified method (1993b)} \quad M_{p, \text{hinge}} = b \frac{f_y t^2}{4} \left[1 - \left(\frac{P}{f_y b t} \right)^2 \right] \quad (2)$$

$$\text{Hiriyur and Schafer (2005)} \quad M_{p, \text{hinge}} = \frac{b}{\cos \beta} \frac{\chi f_y t^2}{4} \left[1 - \left(\frac{P}{\chi f_y b t} \right)^2 \right] \quad (3)$$

where

$$\chi = \frac{\sqrt{3}}{2} + \frac{\cos 2\beta}{2\sqrt{3}} \quad (4)$$

3. Murray's basic yield line mechanisms for flange outstands

Regardless of the method chosen for calculating the capacity of the inclined yield line, the analysis of the spatial plastic mechanism that forms in a flange follows from a consideration of the geometry. Following the equilibrium method of Murray a spatial mechanism may be analysed by considering each component plate in turn. The mechanism that forms in the plate may take different forms depending on the geometry and type of loading that the member is under. A complicated mechanism in a member may therefore be considered as the sum of a number of simple, basic mechanisms in the component plates. Murray and Khoo (1981) analysed eight basic mechanisms, and the inclined yield line that forms in the flange outstand in Fig. 1 considered in this paper, is one half of Murray and Khoo's basic plastic mechanism 5, shown in Fig. 2. This is a true mechanism,

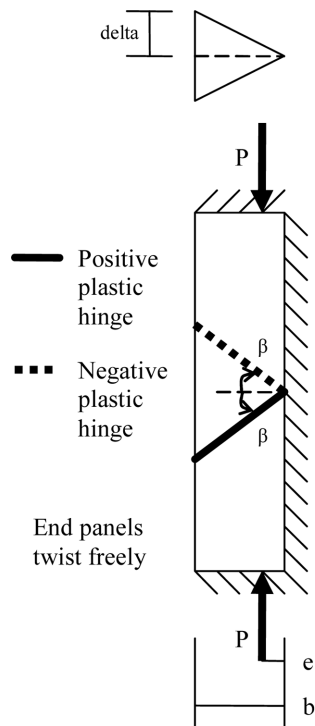


Fig. 2 Murray and Khoo's (1981) true basic mechanism 5

and therefore it is assumed that the loaded edges of the plate may twist freely in the formation of the plastic hinge. Murray's analysis of this mechanism is derived here for the readers convenience, with reference to Fig. 1.

General,

$$M_{p,hinge} = \frac{b}{\cos \beta} \frac{f_y t^2}{4} \left[1 - \left(\frac{P}{f_y b t} \right)^2 \right] \quad (5)$$

$$M_{p,perp} = \frac{M_{p,hinge}}{\cos \beta} \quad (6)$$

$$M_{p,perp} = \sec^2 \beta \frac{f_y t^2 b}{4} \left[1 - \left(\frac{P}{f_y b t} \right)^2 \right] \quad (7)$$

Equilibrium of the longitudinal strip of width dx with central deflection Δ_i in Fig. 1

$$dP \Delta_i = \kappa \frac{f_y t^2}{4} \left[1 - \left(\frac{dP}{f_y t dx} \right)^2 \right] dx \quad (8)$$

where

$$\kappa = \sec^2 \beta \quad (9)$$

solving this quadratic produces

$$dP = f_y t \left[\sqrt{\left(\frac{2\Delta_i}{\kappa t} \right)^2 + 1} - \frac{2\Delta_i}{\kappa t} \right] dx \quad (10)$$

by geometry

$$\Delta_i = \frac{\Delta x}{b} \quad (11)$$

substituting and integrating

$$P = \frac{f_y t b}{2} \left[\sqrt{\left(\frac{2\Delta}{\kappa t} \right)^2 + 1} - \frac{2\Delta}{\kappa t} + \frac{\kappa t}{2\Delta} + \frac{\kappa t}{2\Delta} \ln \left\{ \sqrt{\left(\frac{2\Delta}{\kappa t} \right)^2 + 1} + \frac{2\Delta}{\kappa t} \right\} \right] \quad (12)$$

the moment of P about an axis through the supported edge is found by integrating $x dP$, producing

$$P e = \frac{f_y t^3 b^2 \kappa^2}{12 \Delta^2} \left[\left\{ \left(\frac{2\Delta}{\kappa t} \right)^2 + 1 \right\}^{3/2} - 1 - \left(\frac{2\Delta}{\kappa t} \right)^3 \right] \quad (13)$$

4. Yield line mechanisms in unstiffened plate tests

The unstiffened plate tests of Bambach and Rasmussen (2004a) consisted of rectangular plates simply supported on three sides with the remaining (longitudinal) edge free. The plates were tested under a variety of loaded edge conditions using two actuators simultaneously applying axial load and moment. The loaded edges were constrained to remain straight and displace in-plane, and the

Table 1 Material properties from tensile coupons

Plate	Nominal		Measured		
	$\sigma_{0.2}$ (MPa)	E (GPa)	$\sigma_{0.2}$ (MPa)	σ_u (MPa)	ε_u^1 (%)
1	300	202	271	479	42
2	300	199	317	504	36

¹Based on a gauge length of 50 mm

corresponding load and moment were recorded (displacement control). The loaded edge conditions analysed in this paper are pure compression displacement, compression displacement at the free edge and zero at the supported edge, and compression displacement at the supported edge and zero at the free edge. Since the tested load cases prescribe the applied gradient of displacement, they may be considered as applied strain gradients rather than applied stress gradients. Indeed, in the analysis of Bambach and Rasmussen (2004b) it is shown that after local buckling in slender plates the in-plane stress distribution becomes highly non-linear. Five different slenderness ratios λ (Eq. (14)), where f_{cr} is the elastic critical buckling stress) were tested for each load case, with an average range of values between 0.73 and 2.35, and four plates were tested for each slenderness ratio. Of these, two were welded to induce residual stresses and two were unwelded. The measured material properties of the plates are summarised in Table 1. The plates were tested beyond the ultimate load, and the subsequent post-ultimate load path was recorded down to an average value of 80% of the ultimate load. Further details of the plate tests are presented in Bambach and Rasmussen (2004a), from which reference may also be made for explanation of specimen numbers given in this paper.

$$\lambda = \sqrt{\frac{f_y}{f_{cr}}} \quad (14)$$

In general terms, the plate response involved the formation of one half of a sine wave elastic buckle, with the maximum deflection near the centre of the length of the plate (at the free edge), then as the load reached the ultimate load the buckle deformation localised to one end of the plate forming a plastic hinge (inclined at an angle β) that extended from the supported corner to the free edge, as shown in Figs. 3-6. The mechanism continued to deflect laterally as the in-plane displacement was increased in the post-ultimate range, and additionally the yield line changed

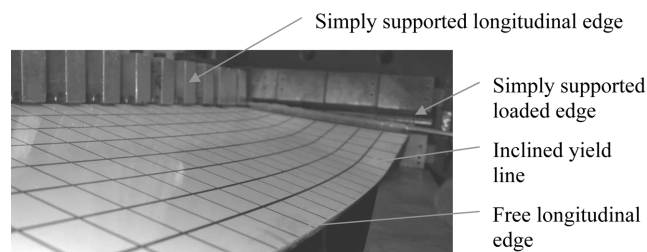


Fig. 3 Typical formation of an inclined yield line in a simply supported rectangular plate with one longitudinal edge free, under in-plane uni-axial compression that is non-uniform across the loaded edge (specimen c12052, $\lambda = 2.35$)

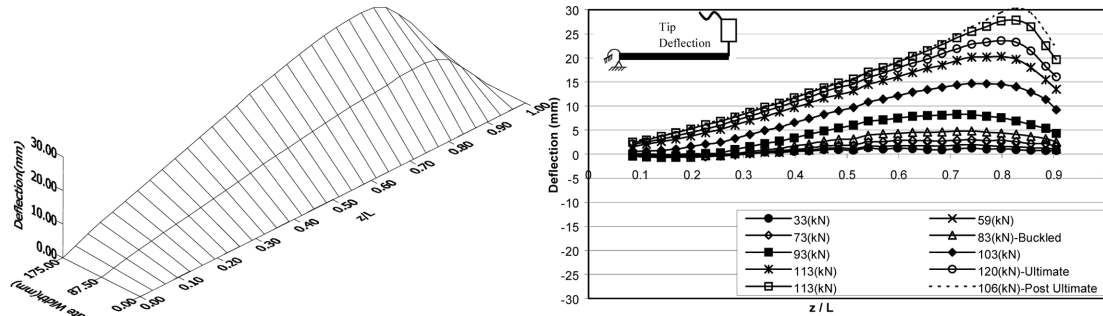


Fig. 4 Displacement profile of unwelded specimen (c01751, $\lambda = 2.17$) under uniform compression displacement at the post-ultimate condition, and plot of the displacement of the free edge

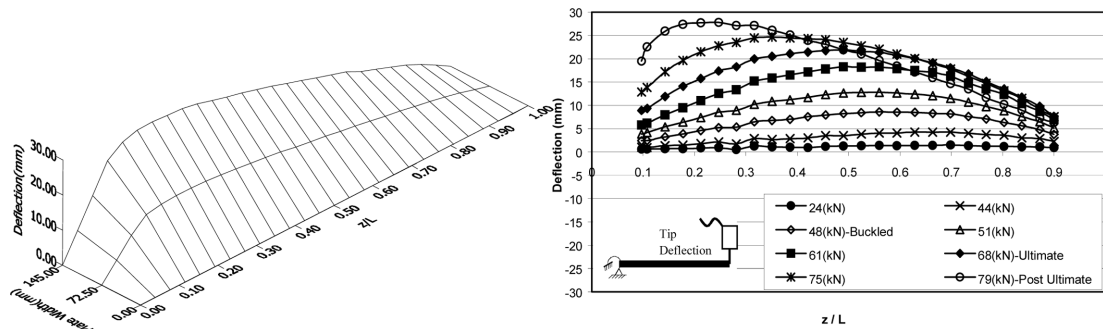


Fig. 5 Displacement profile of unwelded specimen (c11452, $\lambda = 1.54$) under compression displacement at the free edge and zero at the supported edge at the post-ultimate condition, and plot of the displacement of the free edge

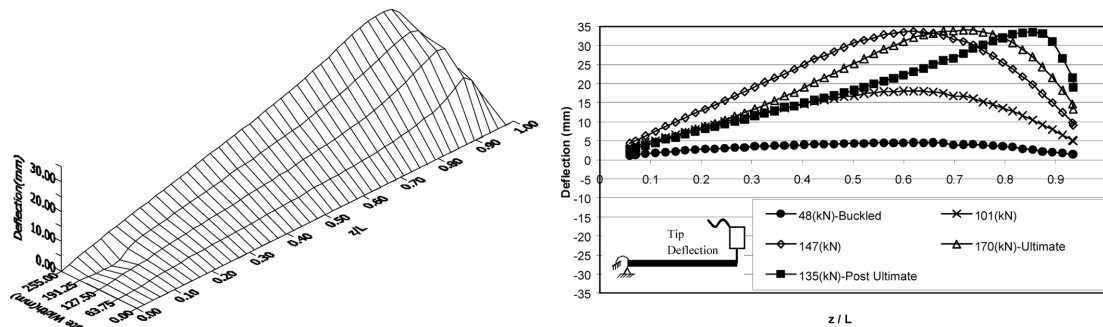


Fig. 6 Displacement profile of unwelded specimen (c32551, $\lambda = 1.69$) under compression displacement at the supported edge and zero at the free edge at the post-ultimate condition, and plot of the displacement of the free edge

inclination slightly as the deformation progressed. The displaced shape is characterised in Figs. 4-6, where a slender plate from each of the three load cases analysed in this paper are presented. It can be seen that the yield line inclination angle, deduced from the position of maximum lateral deflection along the length of the plate (at the free edge), is slightly different for each load case and varies with increasing applied in-plane displacement. Accurate measurements at 25 mm increments along the free longitudinal edge were recorded for at least two of the most slender geometries (i.e.,

Table 2 Average angles of inclination of the yield line to the line of action of the compressive force (β), at ultimate and at post-ultimate (unloaded to 80% of the ultimate load on average)

	Uniform compression displacement	Compression displacement at free edge, zero at supported edge	Compressive displacement at supported edge, zero at free edge
No. specimens	8	8	16
Average β at Ultimate	45.1	62.4	54.8
<i>Std dev</i>	5.4	7.2	9.0
Average β at Post-Ultimate	40.1	50.8	41.1
<i>Std dev</i>	3.6	8.1	5.4
Average β	43	57	48

8 plates in total) in each load case, and the results for the inclination angle of the yield lines are summarised in Table 2. The inclination angle is given at ultimate and at the last recorded value in the post-ultimate range (on average 80% of the ultimate load). The average inclination angle for each load case is used in the analyses in this paper, and is shown in Table 2 to vary between 43° and 57°. The effect of the angle on the results of the yield line mechanism analysis is shown to be quite small in the Appendix of Bambach (2006a), where the model developed in this paper is analysed for angles varying between 40° and 60°.

5. Comparisons of existing theory and plate tests

5.1 General

The results of the plate tests by Bambach and Rasmussen (2004a) were presented as load versus axial shortening curves. For the case of uniform compression displacement the load is the axial force and the axial shortening is the uniform axial displacement. For the load case of compression displacement at the free edge and zero at the supported edge, the load is the total stress at the free edge (Total Stress at the Free Edge in Fig. 7), being the sum of the stress from the compression force and the stress from the bending moment (about the centre width of the loaded edge) at the free edge, and the axial shortening is the axial displacement of the free edge. For the load case of compression displacement at the supported edge and zero at the free edge, the load is the total stress at the supported edge (Total Stress at the Supported Edge in Fig. 9), being the sum of the stress from the compression force and the stress from the bending moment (about the centre width of the loaded edge) at the supported edge, and the axial shortening is the axial displacement of the supported edge. In order to compare the yield line analysis with the plate test results, the lateral displacement of the hinge at the free edge (Δ) must be converted to the axial displacement of the loaded edge (e_{axial}). The equations for the conversion are derived in the Appendix of Bambach (2006a), and the resulting equation is given by Eq. (15). In this equation the elastic axial shortening is also included (Rasmussen and Hancock 1992, Key and Hancock 1986). The yield line analysis provides an axial force (Eq. (12)) and a moment (Eq. (13)) about the supported edge. For the non-uniform compression displacement load cases the moment is converted to a moment about the centre width of the loaded edge, and the stresses from the axial force and moment are deduced and

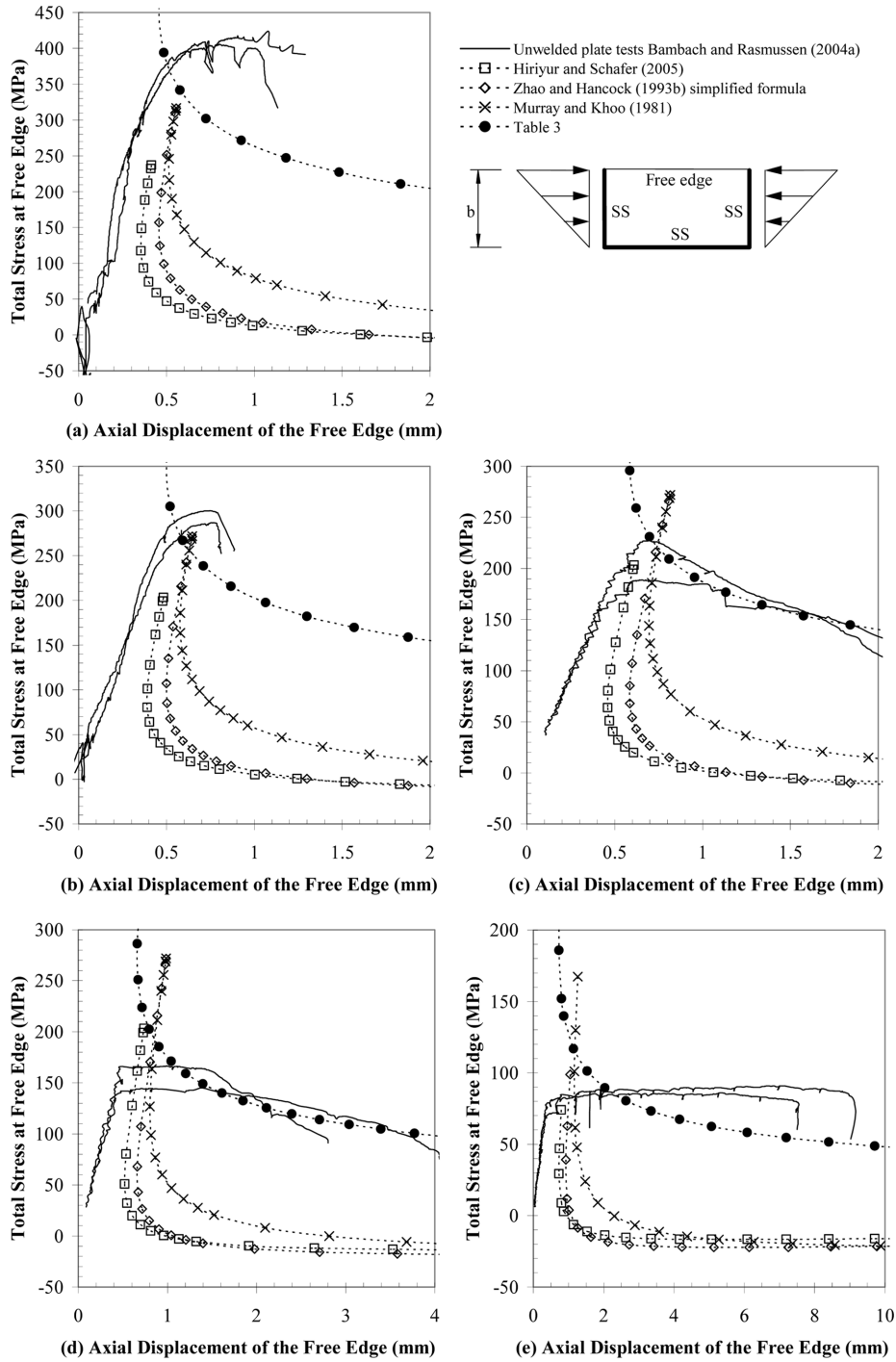


Fig. 7 Total stress at the free edge vs axial shortening of the free edge curves, for unstiffened plates with compression displacement at the free edge and zero at the supported edge – unwelded plate tests compared with theories. Average plate slenderness values are (a) $\lambda = 0.80$, (b) $\lambda = 1.00$, (c) $\lambda = 1.27$, (d) $\lambda = 1.54$, (e) $\lambda = 2.35$. $\beta = 57^\circ$

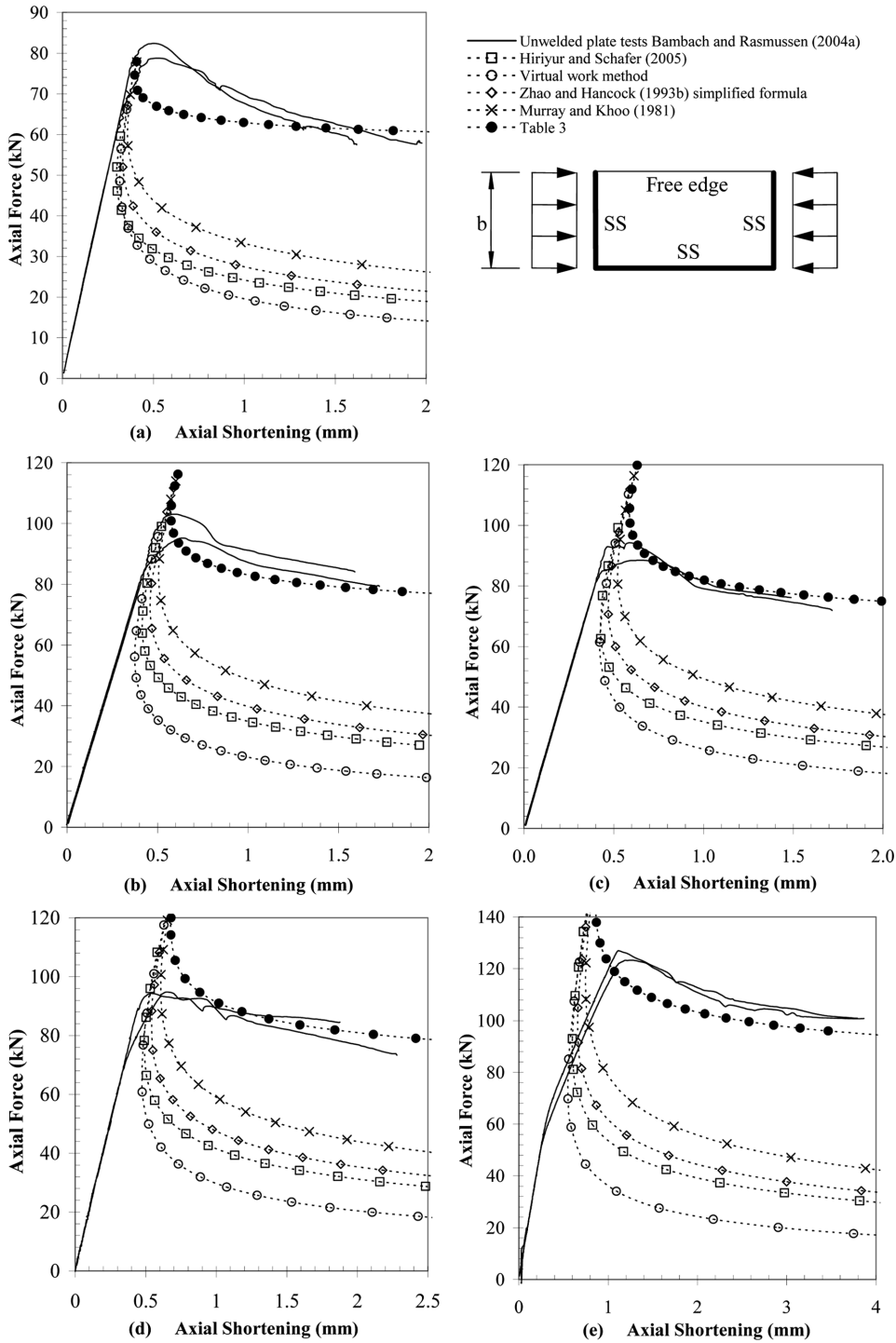


Fig. 8 Axial force vs axial shortening curves for unstiffened plates under uniform compression displacement – unwelded plate tests compared with theories. Average plate slenderness values are (a) $\lambda = 0.76$, (b) $\lambda = 1.08$, (c) $\lambda = 1.25$, (d) $\lambda = 1.57$, (e) $\lambda = 2.17$. $\beta = 43^\circ$

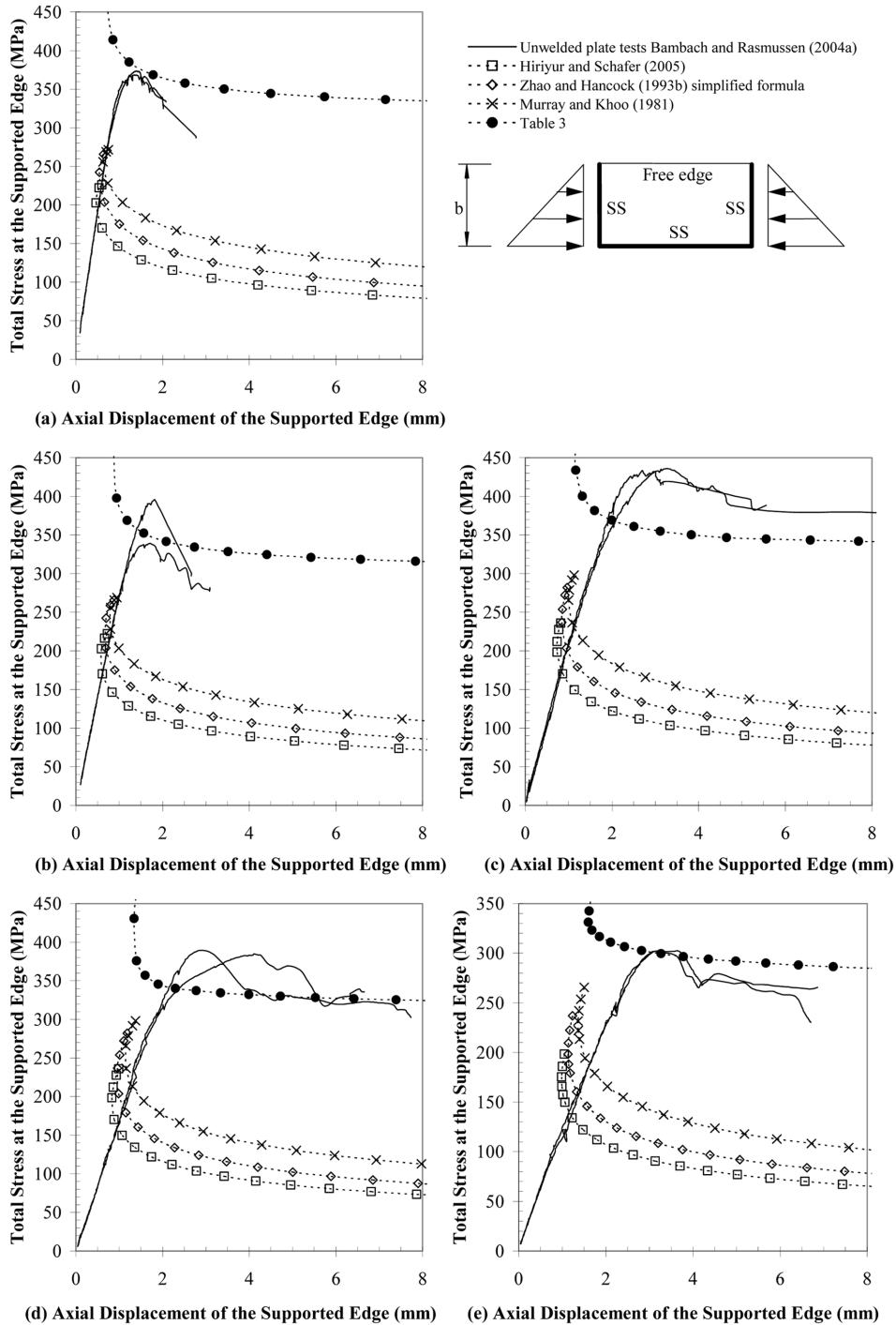


Fig. 9 Total stress at the supported edge vs axial shortening of the supported edge curves, for unstiffened plates with compression displacement at the supported edge and zero at the free edge – unwelded plate tests compared with theories. Average plate slenderness values are (a) $\lambda = 0.73$, (b) $\lambda = 1.01$, (c) $\lambda = 1.36$, (d) $\lambda = 1.69$, (e) $\lambda = 2.35$. $\beta = 48^\circ$

summed. The yield line analysis results are then plotted with the plate test results in Figs. 7-9.

$$e_{axial} = \frac{2\Delta^2}{L} + \frac{PL}{EA} \quad (15)$$

5.2 Plate tests with compression displacement at the free edge and zero at the supported edge

The existing theoretical solutions of Zhao and Hancock (1993b) (Eq. (2)), Hiriyur and Schafer (2005) (Eqs. (3) and (4)) and Murray and Khoo (1981) (Eq. (1)) are compared with the plate tests involving compression at the free edge and zero at the supported edge in Fig. 7. In general terms, it is evident from the graphs that the theoretical methods are very conservative regardless of the slenderness of the plates, however there is a slight trend with slenderness in that the theoretical results for the slender plates are more conservative than those for the less slender plates. It is also clear that while the theories are quite different, in comparison to the inclined yield lines observed in the tests they produce results that are not too dissimilar from each other. Since the existing theoretical results are quite similar and are all very conservative compared to the test results, it is deduced that the conservatism is not a result of the assumed theoretical capacity of the inclined hinge.

5.3 Plate tests with uniform compression displacement

The existing theoretical solutions are compared with the plate tests under uniform compression displacement in Fig. 8. In general terms, it is evident from the graphs that the theoretical methods are quite conservative regardless of the slenderness of the plates, however there is a slight trend with slenderness in that the theoretical results for the stocky plates are more conservative than those for the more slender plates. Again the various theories produce quite similar results, and it is apparent that the general conservatism is not a result of the theoretical method chosen. To investigate whether the virtual work method provides a more accurate solution than the equilibrium method, the static virtual work method is derived in the Appendix of Bambach (2006a) and is compared in Fig. 8. The virtual work method produces a similar result to the equilibrium method and is also conservative for all slenderness ratios tested, and it is therefore apparent that the conservatism is not a result of the use of an equilibrium, rather than a virtual work, approach.

5.4 Plate tests with compression displacement at the supported edge and zero at the free edge

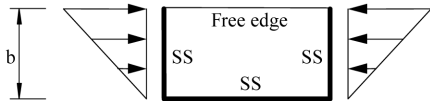
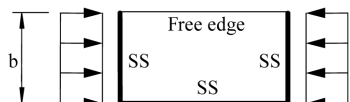
The existing theoretical solutions are compared with the plate tests involving compression at the unsupported edge and zero at the free edge in Fig. 9. In general terms, it is evident from the graphs that the theoretical methods are quite conservative regardless of the slenderness of the plates, however there is a slight trend with slenderness in that the theoretical results for the stocky plates are more conservative than those for the more slender plates. Again the various theories produce quite similar results, and it is apparent that the general conservatism is not a result of the theoretical method chosen.

6. Modified theory

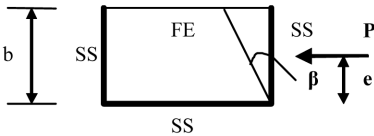
6.1 General

In general terms, the comparisons of the existing theories with the plate tests of the three load cases show that the theories are all quite conservative for all slenderness ratios, and do not match the test data well. It is noted that a similar result was found by Hiriyur and Schafer (2005) in their comparisons with unstiffened plates, where they found that the theoretical mechanism model had little correlation to their finite element model (the capacities calculated were un-conservative when compared with the finite element solution). It is clear that the different theories used for the capacity of the inclined yield line produce quite similar results, and it may therefore be deduced that it is not the assumed hinge capacity that is resulting in the conservatism found for the three load cases. The conservatism may be traced to the assumed mechanism itself, and the treatment of the in-plane displacements that occur at the loaded edges of the plates. In this section modifications of the basic mechanism theory are developed and empirically calibrated to the plate test results, and the resulting methods are presented in Table 3 for all load cases. The assumed hinge capacity in the modified

Table 3 Load (P) and Moment (Pe) resulting from inclined yield lines in flange outstands under various in-plane displacement gradients of the loaded edges

Strain gradient on flange outstand	Load and Moment equations	Factor
	$P = P_1$ $e = \left(0.7 - \frac{\lambda}{25}\right)b$	
	$P = BP_1 + (1 - B)P_y$	$B = \frac{-\lambda^2}{4} + \lambda - 0.3$ $B \geq 0.3$
	$Pe = B^2P_1e_1 + (1 - B)^2P_y\frac{b}{2}$	$B = 0.53 + \frac{\lambda}{10}$

For all load cases:



$$P_1 = \frac{f_y t b}{2} \left[\sqrt{\left(\frac{2\Delta}{\kappa t}\right)^2 + 1} - \frac{2\Delta}{\kappa t} + \frac{\kappa t}{2\Delta} \ln \left\{ \sqrt{\left(\frac{2\Delta}{\kappa t}\right)^2 + 1} + \frac{2\Delta}{\kappa t} \right\} \right]$$

$$P_1 e_1 = \frac{f_y t^3 b^2 \kappa^2}{12 \Delta^2} \left[\left\{ \left(\frac{2\Delta}{\kappa t}\right)^2 + 1 \right\}^{3/2} - 1 - \left(\frac{2\Delta}{\kappa t}\right)^3 \right]$$

$$P_y = f_y b t$$

$$\kappa = \sec \beta$$

$$\lambda = \sqrt{\frac{f_y}{f_{cr}}}$$

This table is valid for slenderness ratios $\lambda \leq 2.35$

theory is taken to be the simplified method of Zhao and Hancock (1993a,b), since it has been the most rigorously verified against test data, and additionally provides a solution that lies between the other two methods analysed in this paper (Figs. 7-9). It is noted that the Zhao and Hancock (1993a,b) method is slightly conservative when compared with Murray and Khoo's (1981) method in Figs. 7-9.

6.2 Plates with compression displacement at the free edge and zero at the supported edge

For the load case of compression displacement at the free edge and zero at the supported edge, the loaded edge of the plate rotates about the supported edge such that the free edge is displacing in-plane and the supported edge is not. This is similar to the condition of the loaded edge in the theoretical model developed earlier in this paper based on Murray and Khoo's (1981) basic plastic mechanism number 5. This mechanism assumes that as the plastic hinge develops the loaded edges of the plate twist freely, resulting in large in-plane displacements at the free edge and little or no displacement at the supported edge, and as such is a true mechanism. The treatment of the loaded edge for this load case is therefore approximately correct, however the results are very conservative in Fig. 7, and indeed the stress at the free edge eventually becomes negative (particularly as the plates become more slender). This is due to the assumed position of the applied load in the mechanism analysis, which results in an assumed stress distribution where the stress is a maximum at the supported edge and linearly decreases towards the free edge. As the mechanism develops the mechanism analysis assumes the applied load moves further towards the supported edge and therefore the stress at the free edge reduces and eventually becomes slightly negative. Analysis of the plates tests for this load case (Bambach and Rasmussen 2004c) shows that the eccentricity of the applied compressive force from the supported edge (e in Figs. 1 and 2) is generally quite large (between $0.56b$ and $0.7b$ from the supported edge). Therefore for this load case the eccentricity in the mechanism analysis is modified, and the expression was deduced by calibration to the plate test results. The resulting (empirical) equation is shown in Table 3. Since the theoretical results became more conservative with increasing slenderness (Fig. 7) it was recognised that the plate slenderness must also affect the capacity, and therefore the slenderness parameter (λ) was included in the equation. The deduced equation was assumed to be linear for simplicity, and was calibrated to the plate test data by adjusting the coefficients (0.7 and $1/25$) until sufficient agreement was obtained with the plate test data for all slenderness ratios for this load case. The resulting equation for the eccentricity in Table 3 produces a result similar to that observed in the plate tests (Bambach and Rasmussen 2004c), where the eccentricity is calculated to be between $0.61b$ and $0.7b$ from the supported edge.

6.3 Plates with uniform compression displacement

If one compares the true mechanism already developed (where the loaded edges of the plate rotate as the yield line develops) to the plates where the loaded edge was displaced uniformly (such that no rotation of the loaded edge occurs), it becomes evident that for the mechanism to form for this load case significant in-plane displacements would need to occur at the supported edge (of equal magnitude to those at the free edge), in addition to the true mechanism. The mechanism that forms for this load case is therefore a quasi-mechanism, and requires a zone of in-plane yielding adjacent

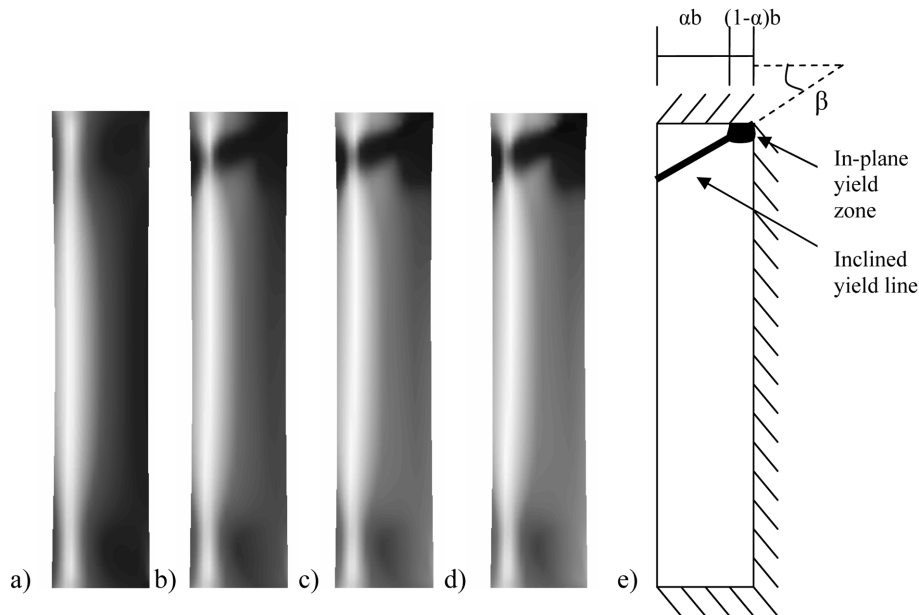


Fig. 10 Ultimate and post-ultimate von Mises (membrane) stress contoured distribution from FEM (Bambach 2006b), at a) ultimate, b) 84% of ultimate, c) 71% of ultimate and d) 66% of ultimate, for plate specimen c01752 under uniform compression displacement, where white is zero stress and black is $1.11f_y$. e) assumed quasi-mechanism (black is the yield stress). In all diagrams the free longitudinal edge is along the left side, and the other edges are simply supported

to the supported edge as the plastic hinge develops. Such an assumption is difficult to verify experimentally, as it was not possible to measure by inspection the size or existence of a yield zone. This assumption was investigated further using the finite element program Strand7. The measured plate geometries including measured geometric imperfections, and the measured material properties (Table 1) were input into the numerical models, and the plates were loaded by displacement control of the loaded edge with the load following directly, as was the case in the experiments. The numerical models were found to be in close agreement with the test results (Bambach 2006b). Having verified the numerical models, the von Mises (membrane) stress distributions were analysed as shown in Fig. 10. In Fig. 10 it can be seen that after ultimate the stresses localise towards one end as the plastic hinge develops there, and the remaining plate areas elastically unload. In addition to the inclined yield line it is clear that an area of in-plane yielding is occurring adjacent to the supported edge. For this load case then, the quasi-mechanism shown in Fig. 10(e) is analysed. Since the width of the yield zone is not known a priori, the model is calibrated against the experimental data, and the resulting (empirical) equation is shown in Table 3 and derived in Appendix A. Limits are applied in Table 3 in order to restrict the values to be within the range of slenderness values in the plate tests. It is noted that in Figs. 10(a)-(d) the maximum stress in the fully developed plastic hinge is 303 MPa, which corresponds to $1.11f_y$ and occurs at a strain of 0.03 on the material curve. No attempt has been made in this analysis to explicitly account for this moderate strain hardening, and the theoretical model assumes the maximum stress is the yield stress. However, since the model has been empirically calibrated to the test data, the effect of strain hardening is nominally included. It is noted that the inclined yield line in the finite element models shown in Figs. 10(a)-(d) has a

zone towards the free edge where the stress is less than that in the remaining areas of the hinge (seen as a lighter area), and this is attributed to the highly non-linear in-plane stress state that occurs in post-buckled slender plates, where the in-plane stress at the free edge of the loaded end where the hinge has formed may become tensile (Bambach 2004b, 2006b).

6.4 Plates with compression displacement at the supported edge and zero at the free edge

For the load case of compression displacement at the supported edge and zero at the free edge, a quasi-mechanism similar to that for the load case of uniform compression displacement is assumed. Again it is clear that significant in-plane yielding must occur adjacent to the supported edge in order for this mechanism to develop. In a similar manner to the uniform compression displacement load case, the width of the yield zone is not known a priori, and the method is therefore calibrated to the experimental results. The resulting (empirical) equation is presented in Table 3 and follows a similar derivation to that in Appendix A.

7. Comparison of modified theory with plate tests

7.1 Plate tests with compression displacement at the free edge and zero at the supported edge

The modified theory deduced in the previous section and presented in Table 3 is compared with the plate tests involving compression displacement at the free edge and zero at the supported edge in Fig. 7. The modified theory approximates the plate test results well, however there are minor discrepancies resulting from using a single linear slenderness function to fit all the test data, which has been used for simplicity. The modified theory clearly matches the test data more closely than the existing mechanism theories.

7.2 Plate tests with uniform compression displacement

The modified theory deduced in the previous section and presented in Table 3 is compared with the plate tests under uniform compression displacement in Fig. 8. Again, the modified theory approximates the plate test results well, however there are minor discrepancies resulting from using a simple polynomial slenderness function to fit all the test data. The modified theory clearly matches the test data more closely than the existing mechanism theories.

7.3 Plate tests with compression displacement at the supported edge and zero at the free edge

The modified theory deduced in the previous section and presented in Table 3 is compared with the plate tests with compression displacement at the supported edge and zero at the free edge in Fig. 9. Again, the modified theory approximates the plate test results well, however there are minor discrepancies resulting from using a simple linear slenderness function to fit all the test data. The modified theory clearly matches the test data more closely than the existing mechanism theories.

8. Application of modified yield line analysis to flanges in sections

In Table 3 the modified yield line mechanism equations are presented for individual flange outstands under three different load cases. When flanges exist in sections, they may be subject to different edge displacement conditions depending on the loads or displacements applied to the section. For open sections in bending, or in compression whereby overall buckling creates bending (i.e., long columns), the flange will be subjected to edge rotation closely approximating the load case of compression displacement at the free edge and zero at the supported edge. It is recommended that for such sections the modified method in Table 3 for flanges with compression displacement at the free edge and zero at the supported edge be used. For open sections in compression whereby overall buckling is not induced (i.e., stub columns), the flange will be subjected to a uniform compression displacement. It is recommended that for fixed ended stub columns the modified method in Table 3 for flanges under uniform compression displacement be used. The third load case in Table 3 of a flange with compression displacement at the supported edge and zero at the free edge is not a commonly developed yield line mechanism in sections, however has been included in this paper for completeness. Having established the appropriate equation for the capacity of the inclined yield line, the analysis of the spatial plastic mechanism that forms in a given application follows from a consideration of the geometry of that mechanism, for example following the equilibrium method of Murray and Khoo (1981) as discussed previously.

9. Conclusions

There exists a variety of solutions in the literature for the capacity of single inclined yield lines, which may form part of the more complex spatial plastic mechanisms that develop in thin-walled steel sections and connections. In this paper various methods have been compared to single inclined yield lines that develop in flange outstands, by comparison with plate tests of plates with three sided simple support, with the remaining (longitudinal) edge free, under uniform and non-uniform in-plane displacement of the loaded edge. It is shown that in the application of the existing theories to flange outstands they produce quite similar results, however they do not match the test data well as the mechanism theory does not account for the in-plane displacement of the loaded edge or the slenderness of the flange outstand. A modified theory has been developed, whereby the in-plane displacement of the loaded edge and the slenderness of the flange are incorporated to produce results for the capacity of the inclined yield line that match the plate test data well. The method is shown to be applicable to flanges that exist in sections, under different nominal load cases such as pure compression for short and long columns, and pure bending.

References

- Bakker, M.C. (1990), "Yield line analysis of post-collapse behaviour of thin-walled steel members", *Heron*, **35**(3), 1-50.
- Bambach, M.R. and Rasmussen, K.J.R. (2004a), "Tests of unstiffened plate elements under combined bending and compression", *J. Struct. Eng., Am. Soc. Eng.*, **130**(10), 1602-1610.
- Bambach, M.R. and Rasmussen, K.J.R. (2004b), "Effects of anchoring tensile stresses in axially loaded plates and sections", *Thin Wall. Struct.*, **42**(10), 1465-1479.

- Bambach, M.R. and Rasmussen, K.J.R. (2004c), "Effective widths of unstiffened elements with stress gradients", *J. Struct. Eng., Am. Soc. Eng.*, **130**(10), 1611-1619.
- Bambach, M.R. (2006a), "Inclined yield lines in flange outstands", *Research Report No. RR2*, Dept. of Civil Engineering, Monash University, Australia, November 2006. Available at <http://civil.eng.monash.edu.au/about/staff/mbambachpersonal>
- Bambach, M.R. (2006b), "Local buckling and post-local buckling redistribution of stress in slender plates and sections", *Thin Wall. Struct.*, **44**(10), 1118-1128.
- Cao, J.J., Packer, J.A. and Yang, G.J. (1998), "Yield line analysis of RHS connections with axial loads", *J. Constr. Steel Res.*, **48**(1), 1-25.
- Davies, P., Kemp, K.O. and Walker, A.C. (1975), "An analysis of the failure mechanism of an axially loaded simply supported steel plates", *Proc. Ins. Civil Eng.*, **59**(2), 645-658.
- Hiriyur, B.K.J. and Schafer, B.W. (2005), "Yield-line analysis of cold-formed steel members", *Steel Struct.*, **5**, 43-54.
- Key, P.W. and Hancock, G.J. (1986), "Plastic collapse mechanisms for cold-formed square hollow section Columns", *Proc. 10th Australasian Conf. on the Mechanics of Structures and Materials*, Adelaide, 217-222.
- Khoo, P.S. (1979), "Plastic local buckling of thin-walled structures", *PhD Thesis*. Monash University.
- Mahendran, M. and Murray, N.W. (1991), "Effect of initial imperfections on local plastic mechanisms in thin steel plates under in-plane compression", *Int. Conf. on Steel and Aluminium Structures*, Singapore.
- Mahendran, M. (1997), "Local plastic mechanisms in thin steel plates under in-plane compression", *Thin Wall. Struct.*, **27**(3), 245-261.
- Mouty, J. (1976), "Calus des charges ultimes des assemblages soudes de profiles creux carres et rectangularies", *Constr. Mettlique.*, **2**, 37-58.
- Murray, N.W. and Khoo, P.S. (1981), "Some basic plastic mechanisms in the local buckling of thin-walled steel structures", *Int. J. Mech. Sci.*, **23**(12), 703-713.
- Murray, N.W. (1984), "Introduction to the theory of thin-walled structures", Oxford: Clarendon Press.
- Murray, N.W. (1973), "Das aufnehmbare Moment in einem zur Richtung der Normalkraft schrag liegenden plastischen Gelenk", *Die Bautechnik*, **50**(2), 57-58.
- Rasmussen, K.J.R. and Hancock, G.J. (1992), "Nonlinear analyses of thin-walled channel section columns", *Thin Wall. Struct.*, **13**(1-2), 145-176.
- Rhodes, J. (2002), "Buckling of thin plates and members—and early work on rectangular tubes", *Thin Wall. Struct.*, **40**(2), 87-108.
- Zhao, X.L. (2003), "Yield line mechanism analysis of steel members and connections", *Prog. Struct. Eng. Mater.*, **5**, 252-262.
- Zhao, X.L. and Hancock, G.J. (1993a), "A theoretical analysis of the plastic-moment capacity of an inclined yield line under axial force", *Thin Wall. Struct.*, **15**(3), 185-207.
- Zhao, X.L. and Hancock, G.J. (1993b), "Experimental verification of the theory of plastic moment capacity of an inclined yield line under axial load", *Thin Wall. Struct.*, **15**(3), 209-233.

Appendix A: Solution of a quasi-mechanism

$$P = \frac{f_y t b}{2} \left[\sqrt{\left(\frac{2\Delta}{\kappa t}\right)^2 + 1} - \frac{2\Delta}{\kappa t} + \frac{\kappa t}{2\Delta} \ln \left\{ \sqrt{\left(\frac{2\Delta}{\kappa t}\right)^2 + 1} + \frac{2\Delta}{\kappa t} \right\} \right]$$

i.e., $P = bC$

With reference to Fig. A1;

$$\begin{aligned} P_{1-2} &= P_1 - P_2 \\ &= (\text{basic mechanism with } b = b_1) - (\text{basic mechanism with } b = b_2) \\ &= b_1 C - b_2 C \\ &= (b_1 - b_2) C \\ &= \alpha b C \quad \text{since } b_1 = b \text{ and } b_2 = (1 - \alpha)b \end{aligned}$$

i.e., basic mechanism with $b = \alpha b$

i.e., $P_{1-2} = \alpha P$

$$P e = \frac{f_y t^3 b^2 \kappa^2}{12 \Delta^2} \left[\left\{ \left(\frac{2\Delta}{\kappa t}\right)^2 + 1 \right\}^{3/2} - 1 - \left(\frac{2\Delta}{\kappa t}\right)^3 \right]$$

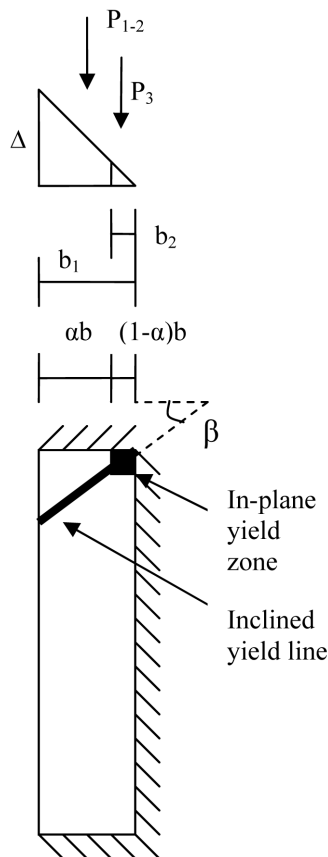


Fig. A1 Quasi-mechanism consisting of a single inclined yield line and an in-plane yield zone, formed in an unstiffened plate with three sides simply supported and the remaining (longitudinal) edge free

Similarly replace b with αb ;

$$P_{1.2}e_{1.2} = \alpha^2 P e$$

$$\begin{aligned} P_3 &= b_2 f_y t \\ &= (1 - \alpha) b f_y t \\ &= (1 - \alpha) P_y \end{aligned}$$

$$\begin{aligned} M \text{ of } P_3 \text{ about supported edge} &= (1 - \alpha)^2 b f_y t (b/2) \\ &= (1 - \alpha)^2 P_y (b/2) \end{aligned}$$

$$\begin{aligned} P_{total} &= P_{1.2} + P_3 \\ &= \alpha^2 P + (1 - \alpha) P_y \end{aligned}$$

$$M_{total} = \alpha^2 P e + (1 - \alpha)^2 P_y (b/2)$$

In the nomenclature of Table 3:

$$P = B P_1 + (1 - B) P_y$$

$$P e = B^2 P_1 e_1 + (1 - B)^2 P_y \frac{b}{2}$$

The factor B is deduced empirically by comparison with the plate test data. Values of B are deduced for each slenderness value, and a linear function is approximated and shown in Table 3.